Nuclear Instruments and Methods in Physics Research B66 (1992) 361–368
North-Holland

Nuclear Instruments & Methods in Physics Research
Section B

Channeling studies of implantation damage in SiGe superlattices and SiGe alloys

M. Vos, C. Wu and I.V. Mitchell
Department of Physics, University of Western Ontario, London, Ontario, Canada, N6A 3K7

T.E. Jackman, J.-M. Baribeau and J.P. McCaffrey
Institute for Microstructural Sciences, National Research Council, Ottawa, Ontario, Canada, K1A 0R6

Received 5 August 1991 and in revised form 13 November 1991

Recent studies have shown a large difference in damage rate between the Si and the SiGe layers of strained-layer superlattices. In order to understand this phenomenon, we have measured amorphisation rates in strained SiGe layers of different composition grown on both Ge and Si substrates and compared these with the damage rates in a pure Si and in SiGe bulk (i.e. strain free) crystals. The combined data suggest that the presence of Ge, rather than the strain, causes the enhancement of the amorphisation rate.

1. Introduction

Ion implantation in semiconductors has been a subject of intensive study in materials science and has been used widely as well in device fabrication for many years. It is therefore surprising that the basic damage production mechanism in Si under the most simple condition, (i.e. self implantation, where impurity effects do not play a role) is still the subject of many recent papers [1–4]. Moreover, theories predicting the dependence of the amorphisation process on parameters such as the total dose, dose rate and temperature are still far from mature.

Concepts used to account for radiation damage in the silicon lattice may be tested by extending them to a related system e.g. SiGe alloys. The use of multilayer epitaxial films of SiGe alternated by pure Si layers allows one to compare the damage rates in Si and SiGe under identical conditions. MBE grown structures of this type may be grown coherently i.e. the strain has not been relieved by misfit dislocations. Thus one should be well aware that in such experiments one introduces strain as much as the alloying impurity into the silicon lattice and it might be that the strain rather than the Ge influences the amorphisation behavior.

We have reported preliminary results of such a study and shown that there is quite a strong enhancement of the amorphisation rate in the SiGe layers compared to the pure Si layers [5]. In this paper we give a more detailed account of these measurements and present new and complementary data obtained from a series of related samples such as $Si/Si_{1-x}Ge_x$ at varying composition x, $Ge/Ge_{1-x}Si_x$ samples, $Si_{1-x}Ge_x$ bulk single crystals and Si and Ge single crystals. The data are examined for evidence that strain plays a role in the amorphisation rate.

2. Experimental details

The $Si/Si_{1-x}Ge_x$ superlattices were grown in a standard molecular beam epitaxy system at a temperature of 500°C on 100 mm diameter Czochralski wafers. Details on wafer preparation and growth are given elsewhere [6]. Ion implantation (with ^{28}Si) and backscattering analysis (with ^4He or ^{11}B) were done at the 1.7 MV Tandetron accelerator of the University of Western Ontario. Use of a tandem accelerator for ^{28}Si implantation has the advantage that no significant amount of N_2 or CO is implanted in the sample. These molecules do have the same mass as ^{28}Si but they can not survive as molecules the electron stripping process in the charge exchange canal of the accelerator. In the first experiment (section 3.1) the Si beam was swept electrostatically over an area of (5×5) mm^2 during Si ion irradiation. In the channeling measurements, the spot size of the analyzing beam was reduced to approximately (2×2) mm^2 to ensure that the analyzed area had been uniformly implanted. A sample temperature rise of a few tens of degrees is expected due to beam heating (beam power $\cong 0.1$ W).

All other implantations (sections 3.2–3.4) used a second target stage with improved temperature control

capabilities. The crystals were clamped onto a copper block and the Si^+ beam was swept over a 2.5 cm diameter aperture. Part of the crystal was covered with Al foil preserving an unimplanted part of the sample for reference during analysis. The dose rate during these implantations was typically 10 to 20 times lower than during the implantations over the (5×5) mm^2 area. The analysis of these samples was subsequently done using a 2 or 3 MeV He^+ beam. In all cases the sample was tilted 7^0 away from the surface normal to minimize channeling effects of the implanted Si ions.

A boron beam was used for some of the analysis of the lattice disorder between subsequent Si irradiations (section 3.1). For these experiments the target of the sputter ion source of the implanter was filled with a mixture of Si and B. In this way implantation of 540 keV $^{28}Si^+$ ions and channeling/backscattering measurements using 3 MeV $^{11}B^{2+}$ ions could be conveniently alternated by appropriate changes of magnetic field and terminal voltage setting. The energy separation of the Si and Ge parts of the RBS spectrum is much larger for ^{11}B ions than for ^4He ions. Detector resolution for MeV B ions is at best about half as good as for He [7], however the stopping power of MeV B in Si is 3 to 5 times larger than that of He ions of the same energy [8]. Thus, using ^{11}B we improve our mass resolution significantly without any loss in depth resolution. The maximum probing depth for 3 MeV B ions in the geometry used is smaller than the range of the 540 keV Si ions and therefore no information could be obtained about the end-of-range damage.

Transmission electron microscopy (TEM) images were taken using a Philips EM 430T electron microscope operating at 250 kV. Samples were prepared using a novel small-angle cleavage technique described elsewhere [9].

3. Results

3.1. The $Si/Si_{0.84}Ge_{0.16}$ multilayer sample

The initial experiments were done on a Si(100) substrate on which 3 pairs of $Si_{0.84}Ge_{0.16}$, with a layer thickness of 275 Å each, alternated by 275 Å thick pure Si were grown. In order to characterize the unimplanted samples, spectra were taken with 2 MeV He^+ ions and the beam aligned close to the ⟨110⟩ axial direction. In fig. 1 we display in a three dimensional plot the intensity of the backscattered particles as a

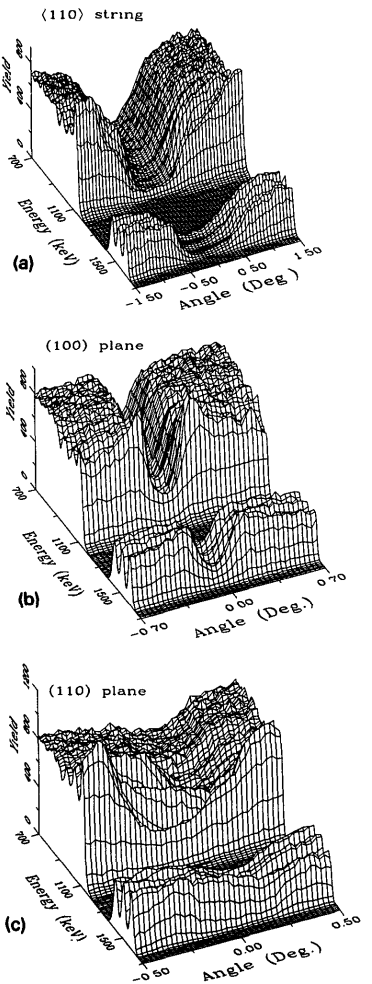

Fig. 1. The dependence of the backscatter yield on sample orientation and energy for a Si/SiGe superlattice. In (a) the alignment was at or close to the ⟨110⟩ string. The three peaks around 1.6 MeV correspond to the Ge in the SiGe layers, the Si edge is at 1.1 MeV. In (b) and (c) we show similar plots for alignment close to the (001) and (1$\bar{1}$0) plane. The (001) plane is not affected by the strain in the superlattice. For the (1$\bar{1}$0) plane there is a difference in the position of the minimum of the surface Si signal and the first Ge layer. This, as well as the large amount of dechanneling, is a consequence of the strain affecting this channeling direction at the interfaces.

function of sample orientation and energy of the detected He^+ ions. The three small peaks at the high energy side are due to Ge in the $Si_{1-x}Ge_x$ layers. As is clear from the strong minimum in the ⟨110⟩ direction for particles backscattered from Ge and Si, the overlayers are indeed epitaxial with the substrate. A minimum yield (X_{min}) of 4% was found, both for the Ge and Si part of the spectra.

A SiGe alloy has a larger lattice constant than pure Si. If a SiGe layer chooses to grow coherently its in-plane lattice constant is equal to that of the Si substrate and the lattice constant in the perpendicular direction will be expanded. Another possibility is that the strain caused by the difference in lattice constants is relieved by misfit dislocations. Planar channeling spectra provide information as to which of the possibilities applies to our samples [10]. Both the $(1\bar{1}0)$ and the (001) plane intersect the ⟨110⟩ string. Similar plots for these directions are shown in fig. 1 as well. Data were taken close to the ⟨110⟩ string, thus all three plots will have similar depth scales. For the (001) plane, which is perpendicular to the surface, a strong minimum is found for both the Si and Ge part of the spectrum. The amount of dechanneling at the interfaces is below the detection limit of these measurements, ruling out the presence of a significant amount of misfit dislocations.

The situation is dramatically different for the $(1\bar{1}0)$ planar direction. The $(1\bar{1}0)$ plane is not perpendicular to the surface. The minima found were not so pronounced, and moreover the Si and Ge minima did not align. This is a well known effect of the strain in epitaxially grown superlattices [10]. The expansion of the SiGe unit cell in the direction perpendicular to the interface will cause a change in direction of the $(1\bar{1}0)$ plane at these interfaces. The change is in this case of the order of the critical angle for channeling, therefore a considerable fraction of the beam will dechannel at the interfaces, causing the channeling effect to be less pronounced for this direction. Also a clear difference of about 0.3^0 in the angular positions was seen for the channeling minima from the outermost Ge layer and the capping pure Si layer. Thus these samples are strained layer superlattices. (These effects are not so easily observed in the case of [110] axial channeling because of its larger critical angle.)

In fig. 2 we show the backscattering spectra, obtained under random orientation and ⟨100⟩ string alignment, after Si implantation doses as indicated. ^{11}B was used as an analysing beam. The 3 peaks in the high energy part of the spectrum are identifiable with ^{11}B particles backscattered from Ge atoms in the $Si_{1-x}Ge_x$ layers. The energy separation of these peaks is 173 keV, in reasonable agreement with the calculated separation (163 keV) for the given geometry (normal incidence, 112.5^0 scattering angle) [8]. In the random spectrum, three small dips in the Si continuum of particles are seen corresponding to the SiGe layers (calculated separation 133 keV, measured 120 keV). X_{min} for 3

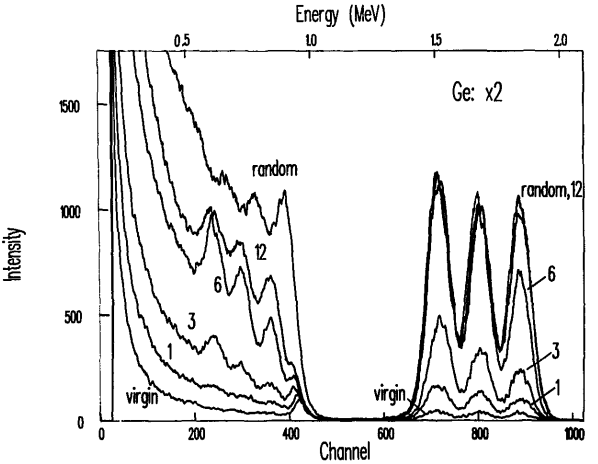

Fig. 2. The gradual increase of the backscattering yield of ⟨100⟩ channeled ^{11}B ions after implantation of 540 keV Si ions. Implantation doses are indicated in units of 10^{14} ion/cm^2. The Ge part of the spectrum is enlarged tweice for clarity. Notice the three distinct disorder peaks in the Si spectrum. For the highest dose the aligned Ge yield is equal to the random value.

MeV ^{11}B ions was $\simeq 4\%$ (for both the Ge and Si part of the spectrum) which is typical for B channeling in pure Si [11].

After implantation of 1.0×10^{14} Si ions/cm^2 an increase was observed in the aligned backscattering yield which increased with increasing depth. This does not necessarily mean that the level of disorder increases with depth: the increase of the yield at any depth is due to backscattering of the channeled B ions by defects at that depth, plus the scattering contribution of ions dechanneled as a consequence of all defects present at smaller depth [12,13].

At a larger Si implantation dose (3.0×10^{14} Si ions/cm^2), three peaks appeared in the Si part of the spectrum at energies closely matching those of the minima in the random spectrum, i.e. they correspond to the SiGe layers. Clearly, the backscatter yield from Ge has increased with implantation dose as well and at a comparable rate. The increase in the yield from the pure Si layers and substrate was slower. Thus the SiGe layers have been preferentially damaged.

At a dose of 6.0×10^{14} Si ions/cm^2 the yield of the deeper Ge peak was indistinguishable from the random yield. The conventional interpretation of such a saturated channeling disorder signal is amorphisation. The yield in the Si part of this SiGe layer is not completely equal to the random yield due to the finite detector resolution. At a fluence of 1.2×10^{15} Si ions/cm^2 the aligned yield from all the Ge layers was equal to the random yield.

Independent evidence for the amorphisation of the SiGe layers is obtained from the cross sectional transmission electron microscopy (TEM) measurements as published in ref. [5].

In order to be sure that the B ions did not contribute to the observed changes in the superlattice crystallinity, another sample was irradiated with 3 MeV B ions up to a dose of 2.0×10^{16} ions/cm^2. Only a slight increase was observed in the X_{min} of both Si and Ge (from 4% to ~ 7%). The actual dose of the analyzing B ion beam after each irradiation step did not exceed 3.0×10^{15} ions/cm^2. Thus we are confident that the effects observed are almost exclusively due to the Si implantation.

The rise in the yield from the Si substrate after the implantation of 1.2×10^{15} Si$^+$ ions will be in part due to implantation damage in the substrate and in part due to dechanneling of the B beam in the amorphous SiGe layers. In order to get some feeling for the ratio of both contributions we performed Monte Carlo computer simulations. As published elsewhere such simulations give an excellent description of the channeling of MeV B$^+$ ions in Si [11]. The simulations were done for a pure Si crystal with three amorphous Si layers of 275 Å thickness alternated by three crystalline Si layers in a way similar to the MBE grown and implanted superlattice. Thus the effect of Ge in the amorphous layers was neglected. In the amorphous layers the impact parameter for following collisions was chosen randomly, while care was taken that the densities of the amorphous and crystalline Si layers were identical. From the simulations a spectrum was calculated using stopping power values and detector response functions as described in [11]. The result is shown in fig. 3. Qualitatively the measured and simulated spectra are similar, thus defects in the Si substrate are not the major cause of the increase in B backscattered yield below the deepest SiGe layer. However defects certainly will be present and enhance the yield in a minor way.

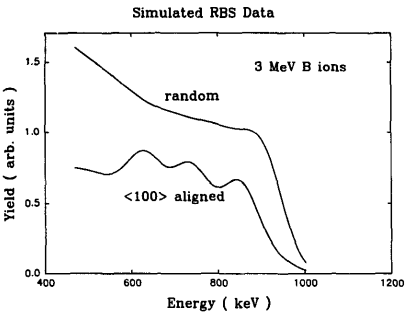

Fig. 3. A simulation of a channeling spectrum for a pure Si crystal with three amorphous layers of 275 Å thickness, at depth equal to the depth of the SiGe layers of fig 2. From this simulation we find a large increase in backscatter yield from the Si at depths exceeding the last amorphous Si layer, due to dechanneling.

In turned out that the amorphous layers regrew after annealing of the sample at 550°C [5]. An important question is if the strain would regrow in the Ge layers or would be relieved by defects (misfit dislocations). Therefore we measured the angular dependence of the backscatter yield of the implanted part of the sample after annealing at 550°C and compared this with the yield of the virgin part of the sample. These measurements were done for the (110) plane close to the $\langle 1\bar{1}0 \rangle$ string. As discussed for fig. 1 these measurements are sensitive to the presence of strain. 2 MeV He$^+$ ions, rather than 3 MeV B^{2+} ions were chosen because of their smaller channeling half angles, and therefore greater sensitivity to the presence of strain. The scattering yield from the capping Si layer is plotted together with the yield of the first (closest to the surface) SiGe layer in fig. 4. The outermost layers were chosen because in that case the steering effects of the different layers with different strain on the He beam is

the least disruptive. As is clear from fig. 4 the difference in the position of the minimum is about 0.3° both for the as grown sample and for the implanted and subsequently annealed one, i.e. strain has been re-established in the regrown lattice.

Other studies have been published on the regrowth of strained layers [14]. In that case the samples were amorphised all the way from the surface to the end of range of the Si ions. For Ge concentrations similar to the one reported here they also found a regrowth of the strain in the SiGe layers, after solid phase epitaxial regrowth of the amorphous layer.

3.2. Implantation in single layers of $Si_{1-x}Ge_x$ on a Si substrates

Further examples of the enhancement of the implantation damage in MBE grown SiGe layer are presented in fig. 5. Here single layers of an $Si_{1-x}Ge_x$ alloy were grown on a Si(100) wafer and subsequently implanted with 540 keV Si ions. One sample had a 1500 Å SiGe layer with composition $Si_{0.90}Ge_{0.10}$. The other sample had an 1800 Å thick SiGe layer with composition $Si_{0.85}Ge_{0.15}$. They were implanted simultaneously, side by side. The implanted dose was 2.0×10^{15} /cm^2 at an energy of 540 keV (2.5 cm implantation area

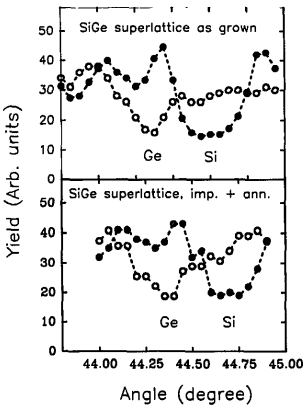

Fig. 4. The angular dependence of the backscatter yield for the outer, pure Si layer as well as the Ge yield of the first SiGe layer. The difference in position of the minima is a consequence of the strain. After selective amorphisation of the SiGe layers, followed by epitaxial regrowth of these layers, the same amount of strain is found, although the minima are slightly less deep, indicating the presence of some residual damage.

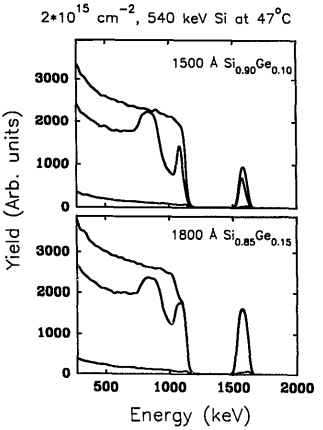

Fig. 5. Damage build up after implantation in a thick (> 1000 Å) single layer of SiGe on a Si substrate. Implantation dose was 2×10^{15} Si ions/cm^2 at a temperature of 320 K. A 2 MeV He^+ beam was used as an analysing beam. The layer with a Ge concentration of 15% is completely amorphised whereas the Ge layer of 10% is preferentially damaged, but not yet completely amorphised.

diameter, ~300 nA current, sample mechanically clamped on a Cu block) The implantation temperature chosen was 320 K in order to mimic the beam heating effect in the multilayer experiment (section 3.1). The larger dose necessary to obtain amorphisation in the $Si_{0.85}Ge_{0.15}$ in this case compared to section 3a is due to the lower dose rate [4]. Again the layer with highest Ge concentration is amorphised first but even at 10% Ge there is a strong enhancement of the damage relative to pure Si. If one compares quantitatively the damage in the Si substrate and Ge overlayer one should correct for the increasing amount of dechanneling with increasing depth [10]. If one performs the decomposition of the increased backscatter yield into dechanneling and direct scattering contributions as described elsewhere [12,13], one obtains a damage level in the 10% Ge layer that is 3 times higher than in the Si directly below the SiGe layer. This enhancement is about 4 times for the 15% Ge layer. Notice that at the end of range of the Si ions where the number of atomic displacements is largest the substrate of the 10% alloy has almost reached the random (i.e. amorphous) level, whereas the RBS signal from the substrate of the 15% sample is still well below the amorphous level. This was probably caused by slight differences in thermal contact between both samples, and is a clear example of

the sensitivity to the temperature of the implantation damage. Note that, in spite of the possibiliy of a somewhat higher temperature for the 15% sample its SiGe layer was amorphised.

These samples were subsequently analysed by cross sectional TEM. The TEM images are shown in fig. 6. These images nicely confirm the interpretation of the RBS/channeling data. The 15% alloy is amorphous over the whole SiGe layer (with the exceptions of some tiny crystallites near the surface). The 10% sample seems amorphous only directly at the interface, and the near surface region still has a clear crystalline character. In between there is a zone that appears in the TEN image to be polycrystalline. Thus the TEM images confirm the interpretation of the RBS/channeling spectra.

3.3. Strained Si_xGe_{1-x} layer grown on a Ge(100) wafer

In order to get some insight into the role of strain on the amorphisation process we irradiated a Ge sample having a Si_xGe_{1-x} ($x \cong 0.20$) layer of 1300 Å grown on top with 3 MeV Si ions. For pure Ge the amorphisation dose is much lower than for Si. Implantation of 1×10^{14} ions/cm^2 caused a high damage concentration at the end of range of the Si ions (1.6 μm). Close to the surface the Ge signal from the 1300 Å thick SiGe layer did not reflect any enhanced damage rate compared to the Ge at a little greater thickness. Thus in the inverse case (SiGe grown on a Ge substrate) no preferential amorphisation is found for the strained layer.

3.4. Implantation in bulk SiGe crystals

Two bulk SiGe crystals (orientation (111), of rather poor quality compared to Si wafers as indicated by a minimum yield of 16% for He^+ ions channeling in the 111 axial direction) and having Ge concentrations of 2 and 7% were implanted with Si^+ ions at 540 keV. The dose was 1.0×10^{15} /cm^2 (implantation area 2.5 cm diameter, implantation current 300 nA, sample mechanically clamped on a copper block). Damage produced in these samples is compared with the implantation damage in a Si(100) wafer in fig. 7. The Si crystal implanted under the same conditions has a 70% defect concentration. For the 2% alloy the height of aligned Ge signal, at the depth corresponding to the range of the Si^+ ions, is equal to the random level within the accuracy of the measurements. Thus the crystal was amorphous at the end of range of the Si ions. The 7% Ge alloy was amorphised over a much larger depth range than the 2% alloy.

This is not the case for the peak corresponding to Si signal from the end of range of the ions, because superimposed on this signal is a contribution of Ge from large depth, that of course will display a channeling effect. As a caveat we have to say that because of the extreme sensitivity of the damage to implantation conditions some of the differences may be caused by

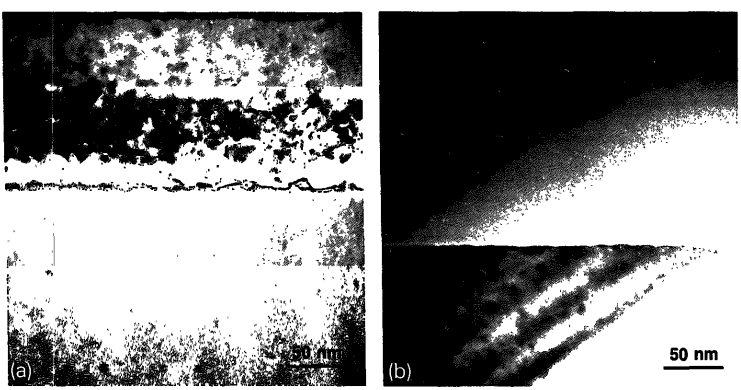

Fig. 6. Cross-sectional TEM pictures of the same samples as fig. 6. The surfaces are at the top of the photographs. In the TEM image the 10% alloy (a) seems amorphous in a narrow region (1500 Å) near the interface, followed by a layer that appears polycrystalline. Close to the surface this layer is still crystalline with some defects, as is the Si substrate directly below the interface. The 1800 Å layer 15% alloy (b) is amorphous except for some tiny crystallites near the surface.

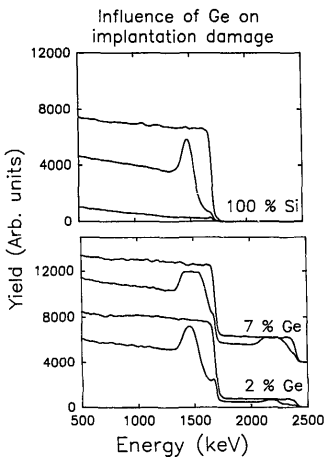

Fig. 7. The dependence of the damage production on the Ge concentration in strain free bulk Ge crystals. All samples were implanted at RT with 1×10^{15} /cm^2 540 keV Si ions. 3 MeV He^+ was used as an analysing beam. An increase in damage with increasing Ge concentration is found.

differences in the thermal contact of the samples with the sample holder. Experiments were repeated on a somewhat different sample holder, and revealed the same general trend. Thus we think that the enhanced amorphisation rate in the MBE grown samples is a consequence of the Ge concentration rather than the strain.

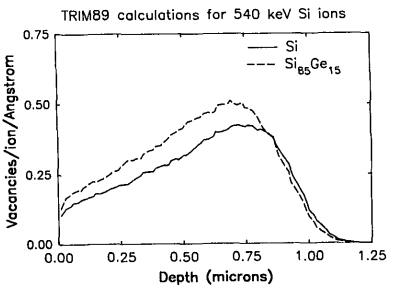

Fig. 8. TRIM calculation of the total vacancy production for implantation in pure Si and a $Si_{85}Ge_{15}$ alloy. The initial vacancy density is about 20% larger in the alloy compared to pure Si.

4. Conclusions and discussion

A clear enhancement was found of the damage production in SiGe layers relative to Si. From the measurements on a strained SiGe layer grown on Ge as well from the results of the bulk SiGe crystal it seems that strain is not the primary cause of this enhancement. The most obvious difference between implantation in Si and SiGe arises from the higher atomic number of Ge. Since the Rutherford cross section is larger the displacement probability in the SiGe layer will be larger. A plot of the defect production as calculated using TRIM is shown in fig. 8. The total vacancy production is somewhat larger (~ 15%) for the $Si_{85}Ge_{15}$ case relative to pure Si. Also the range is somewhat smaller (5%) causing the total damage cascade to be approximately 20% more dense. From implantation studies using molecular species instead of single ions it is known that the damage retained after implantation is very sensitive to this cascade density [15]. Whether this 20% increase in density is enough to explain the 4-fold increase in retained damage is a question open for debate. The damage retained in Si after implantation near RT is very sensitive to variables such as dose rate and implantation temperature [4]. Thus the damage retained is not simply related to the initial damage production, but thermal properties of the defects produced seem to be important as well. It might well be that the presence of Ge influences these properties in a way that leads to an additional enhancement of the damage retained in the sample.

Eaglesham et al. reported similar experiments of low temperature Si implantation in superlattices of group IV and III–V materials [16]. In contrast to the III–V materials they found that the rate of damage production in group IV materials was not affected by the distance to the interfaces. Their group IV superlattices were grown on a GeSi buffer layer in which the strain was (partially) accommodated by misfit dislocations, and consequently strain was also present in the Si layers of the superlattice. Again they found selective amorphisation of the SiGe layers. These findings are in agreement with our conclusion that the preferential amorphisation is a consequence of the presence of Ge rather than strain (or the presence of interfaces).

Acknowledgements

The authors want to thank G. Mulligan for the operation of the accelerator. This research is funded in part by the Ontario Center for Materials Research.

References

[1] T. Motooka, and O.W. Holland, Appl. Phys. Lett. 58 (1991) 2360.
[2] N. Hecking, K.F. Heidemann and E te Kaat, Nucl. Instr. and Meth. B15 (1986) 760.
[3] J.M. Poate, S. Coffa, D.C. Jacobson, A. Polman, J.R. Roth, G.L. Olson, S. Roorda, W. Sinke, J.S. Custer, M.O. Thompson, F. Spaepen and E. Donovan, Nucl. Instr. and Meth. B53 (1991) 533.
[4] P.J. Schultz, C. Jagadish, M.C. Ridgway, R.G. Elliman and J.S. Williams, Phys. Rev. B44 (1991) 9118.
[5] M. Vos, C. Wu, I.V. Mitchell, T.E. Jackman, J.-M Baribeau and J. McCaffrey, Appl. Phys. Lett. 58 (1991) 951.
[6] J.-M. Baribeau, T.E. Jackman, D.C. Houghton, P. Maigné and M.N. Denhoff, J. Appl. Phys 47 (1988) 5738.
[7] P.F. Hinrichsen, D.W. Hetherington, S.C. Gujrathi and L. Cliche, Nucl. Instr. and Meth. B45 (1990) 275.
[8] J.F. Ziegler, J.P. Biersack and U. Littmark, The Stopping and Range of Ions in Solids (Pergamon, New York, 1985).
[9] J.P. McCaffrey, Ultramicroscopy 38 (1991) 149.
[10] S.T. Picraux, W.K. Chu, W.R. Allen and J.A. Ellison, Nucl. Instr. and Meth. B15 (1986) 306.
[11] M. Vos, C. Wu, I.V. Mitchell and P.J.M. Smulders, Nucl. Instr. and Meth. in press (14th Int. Conf. on Atomic Collisions in Solids, Salford UK, 1991).
[12] L.C. Feldman, J.W. Mayer and S.T. Picraux, Materials Analysis by Ion Channeling (Academic Press, New York, 1982).
[13] P.J. Simpson, M. Vos, I.V. Mitchell, C. Wu and P.J. Schultz, Phys. Rev. B44 (1991) 12180.
[14] B.T. Chilton, B.J. Robinson, D.A. Thompson, T.E. Jackman and J.-M. Baribeau, Appl. Phys. Lett. 54 (1989) 42.
[15] J.A. Davies, G. Foti, L.M. Howe, J.B. Mitchell and K.B. Winterbon, Phys. Rev. Lett. 34 (1975) 1441.
[16] D.J. Eaglesham, J.M. Poate, D.C. Jacobson, L.N. Pfeiffer and K. West, Appl. Phys. Lett. 58 (1991) 523.